

Analysis of dependency current harmonics on load and filter parameters for asymmetrical network models

Abstract. The paper presents the operation of three-phase magneto conjugate LCL-filters used in inverter systems of solar power plants. The purpose of their usage is maintaining the coefficient of load current harmonics within the limits imposed by electric power quality standards. As opposed to widespread LC-filters, the LCL-filters enable using of an inverter system for operation in reverse mode at night to charge the batteries of solar power plants. In its turn, the structural design of filter inductances in the form of a three-leg magnetic system that generates magnetic coupling between inductances of different phases ensures the reduction of filter dimensions and its cost. Filter's transfer characteristic was generated and on its basis plotted were dependencies between the current harmonics coefficient and the load, as well as network power coefficient and filter parameters. Analysis of these dependencies demonstrated the availability of composite resonance of currents in the circle, with the greatest resonant currents (and at the same time harmonics coefficients) being observed at light network loads. Considerable restriction of the current harmonics coefficient may be achieved by regulating the filter capacity depending on inductances and power coefficients.

Streszczenie. W artykule przedstawiono działanie trójfazowych filtrów LCL ze sprzężeniem magnetycznym stosowanych w systemach inwerterowych elektrowni słonecznych. Celem ich zastosowania jest utrzymanie współczynnika harmonicznego prądu obciążenia w granicach narzuconych przez normy jakości energii elektrycznej. W przeciwieństwie do powszechnie stosowanych filtrów LC, filtry LCL umożliwiają wykorzystanie systemu inwerterowego do pracy w trybie rewersyjnym w nocy, do ładowania akumulatorów w elektrowniach słonecznych. Z kolei konstrukcja indukcyjności filtracyjnych w postaci trójstopniowego układu magnetycznego generującego sprzężenie magnetyczne pomiędzy indukcyjnościami różnych faz zapewnia redukcję wymiarów filtra i jego kosztów. Określono charakterystykę przenoszenia filtra i na jej podstawie wyznaczono zależności pomiędzy współczynnikiem bieżącej harmonicznej a obciążeniem, a także współczynnikiem mocy w sieci i parametrami filtra. Analiza tych zależności wykazała, że największe prądy rezonansowe (a jednocześnie współczynniki harmonicznego) obserwowano przy niedużych obciążeniach sieci. Znaczne ograniczenie współczynnika harmonicznego prądu można osiągnąć poprzez regulację pojemności filtra w zależności od indukcyjności i współczynników mocy. (Analiza zależności harmonicznego prądu od obciążenia i parametrów filtrów dla modeli sieci).

Keywords: LCL filters, current harmonics, solar power plants.

Słowa kluczowe: filtry LCL, harmoniczne prądu, elektrownie słoneczne.

Introduction

Rapid development of solar power industry in recent decades rekindled the interest in further improvement of systems for inversion of the direct voltage generated by solar batteries into three-phase sinusoid network voltage.

In order to maintain coefficient of load current harmonics within tolerable limits not exceeding 3%, the filter is switched on after the inverter. LC-filters are the most commonly encountered in the inversion systems [1,2,3].

At the same time, for more stable operation of present-day solar power plants, these are equipped with accumulator batteries being charged from network at night. To ensure the possibility of a reverse mode of operation, LCL-filters are increasingly employed in inversion systems [4-6].

Besides, in order to reduce the dimensions and the cost of such filters, they are designed in the form of a three-leg magnetic system having magnetic coupling between inductances of different phases [7-11]. In this paper, we will consider the functioning of this very filter.

Mathematical model of magneto conjugate LCL-filter

The goal of this paper is to generate and analyze the dependencies between current's non-linear distortion coefficient and load with different network power coefficients and filter parameters. The circuit of three-phase magneto conjugate LCL-filter is shown in fig. 1.

For that purpose, let us first find out the AFC of filters in relation to load current. According to the compensation theorem, the equivalent load will be represented as $Z_n = R_n + j\omega L_n$

Since the three-phase filter circuit may be deemed symmetrical, to simplify the task we will determine the AFC for a single-phase filter (fig. 2).

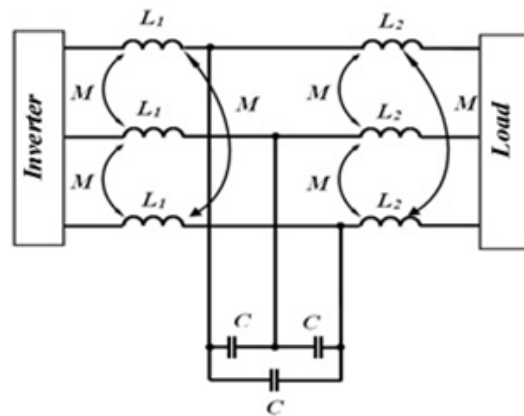


Fig.1. Three-phase magneto conjugate LCL-filter circuit

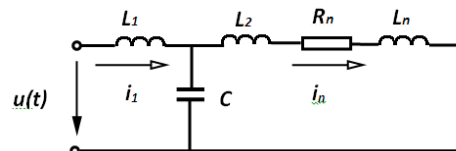


Fig. 2 – Single-phase LCL-filter circuit

Filter's AFC in relation to the load current represents the module of transfer characteristic [7]:

$$(1) \quad H_{iu}(j\omega) = \frac{L_n(j\omega)}{U(j\omega)}$$

In order to determine the same, let us first find out the input resistance of the circle, taking into account the magnetic couplings with other phases. Note that $M = k_z L$, where k_z – magnetic coupling ratio [8].

In general terms, this may be written as follows:

$$(2) \quad Z_{ex}(j\omega) = Z_1(j\omega) + \frac{Z_2(j\omega) \cdot Z_3(j\omega)}{Z_2(j\omega) + Z_3(j\omega)};$$

where $Z_1(j\omega) = j\omega(L - K_1 k_z L a - K_2 k_z L a^2)$;

$$Z_2(j\omega) = \frac{1}{j\omega C};$$

$$Z_3(j\omega) = R_n + j\omega\left(\frac{L}{2} - K_1 k_z \frac{L}{2} a - K_2 k_z \frac{L}{2} a^2 + L_n\right);$$

$a = e^{j120^\circ}$ – the turnaround coefficient that accounts for difference between current phases of neighboring inductances;

$K_1 = k_1 e^{j(\varphi - \varphi_1)}$, $K_2 = k_2 e^{j(\varphi - \varphi_2)}$ – the coefficients that account for the difference between complex values of currents of neighboring inductances.

Then the input current

$$(3) \quad I_1(j\omega) = \frac{U(j\omega)}{Z_{inp}(j\omega)},$$

and the load current

$$(4) \quad I_n(j\omega) = I_1(j\omega) \frac{Z_2(j\omega)}{Z_2(j\omega) + Z_3(j\omega)}.$$

Hence, the circle's transfer characteristic in relation to the load current (1), taking into account expressions (2), (3), (4) is written as follows:

$$(5) \quad H_{iu}(j\omega) = \frac{Z_2(j\omega)}{Z_{inp}(j\omega) \cdot [Z_2(j\omega) + Z_3(j\omega)]}.$$

Since capacities of three-phase filter are connected by a triangle, their values should be translated into an equivalent star.

$$\frac{1}{j\omega C_{star}} = \frac{1}{\frac{j\omega C_{triangle}}{j\omega C_{triangle}} + \frac{1}{\frac{j\omega C_{triangle}}{j\omega C_{triangle}} + \frac{1}{j\omega C_{triangle}}}} = \frac{1}{\frac{j^2 \omega^2 C_{triangle}^2}{3} + \frac{1}{j\omega C_{triangle}}}, \text{ hence } C_{star} = 3C_{triangle}.$$

The equivalent load resistance is determined using the

$$\text{formulae: } Z_n = \frac{U_{ph}}{I_{ph}}, \quad R_n = Z_n \cos(\varphi_n),$$

$$X_n = Z_n \sqrt{1 - \cos^2(\varphi_n)}, \quad L_n = \frac{X_n}{2\pi f}.$$

where U_{ph} – active phase load voltage; I_{ph} – active phase load current; $\cos(\varphi_n)$ – load power coefficient.

The spectrum of post-inverter active values of phase voltage U_{kf} from the 1st to the 50th harmonics set as percentage of the first harmonic is obtained from the

measurement devices or (in the absence of devices) according to the results of computer modeling.

Given that in a three-phase circle with no zero wire, currents of harmonics multiple of three are equal to zero, the spectrum of currents in the load is determined using the expression:

$$(6) \quad (\forall k = 1 \dots 50) \left\{ \begin{array}{l} [(k = 3m) \Rightarrow (I_{kn} = 0)] \vee \\ \vee [(k \neq 3m) \Rightarrow (I_{kn} = U_{kf} |H_{iu}(jk\omega)|)] \end{array} \right\}.$$

And finally, for current harmonics coefficient THD may be written as follows:

$$(7) \quad THD = \frac{\sqrt{\sum_{k=2}^{50} I_{kn}^2}}{I_{1n}}.$$

Results of analysis of THD(I) dependencies with different network $\cos(\varphi)$ and filter parameters

THD(I) dependencies were plotted using the above formulae in MathCAD.

Multiple calculations of THD(I) dependencies were carried out during the investigation, but the limited size of the article does not allow setting them forth. Thus let us restrict ourselves with the most specific results.

First of all, calculations are set forth for the filter with the following parameters: $L_1 = 100\mu\text{H}$, $k_z = 0.5$, $C = 600\mu\text{F}$ (corresponding to 200 μF of capacity connected in a triangle) for network $U_{ph} = 220\text{V}$, $f = 50\text{Hz}$ with a weak amplitude asymmetry $k_1 = 0.9$, $k_2 = 1.1$ and absence of phase asymmetry $\cos(\varphi) = \cos(\varphi_1) = \cos(\varphi_2) = 0.98$.

The diagram is shown in fig. 3.

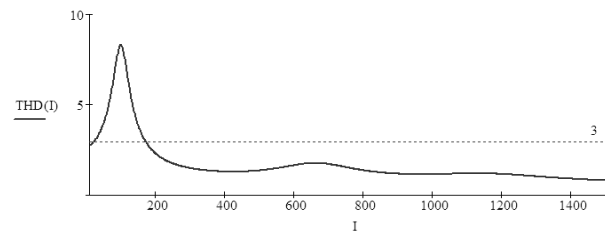


Fig. 3. THD(I) diagram ($k_1 = 0.9$, $k_2 = 1.1$, $\cos(\varphi) = \cos(\varphi_1) = \cos(\varphi_2) = 0.98$)

Quite a considerable resonance (i THD) at light loads can be readily noticed. Let us consider how phase asymmetry influences this dependency. For example, a weak phase asymmetry $\cos(\varphi) = 0.98$, $\cos(\varphi_1) = \cos(\varphi_2) = 0.95$ causes a sharp increase of THD (fig. 4), while a remarkable phase asymmetry $\cos(\varphi) = 0.98$, $\cos(\varphi_1) = \cos(\varphi_2) = 0.85$ makes it possible for all loads to fulfill $THD \leq 3\%$ condition (fig. 5).

Should power coefficients be different for each phase, the advantageous effect will be observed, when the phase with the greatest amplitude has lesser $\cos(\varphi_n)$, as is clear from fig. 6.

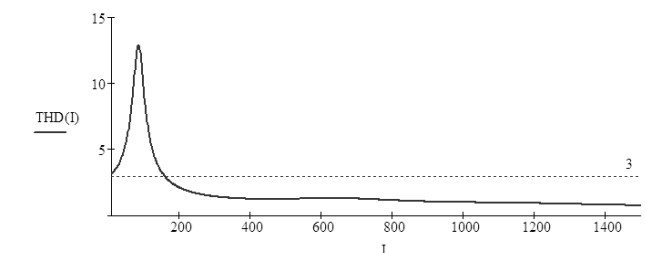


Fig. 4. THD(I) diagram ($k_1 = 0.9$, $k_2 = 1.1$, $\cos(\varphi) = 0.98$, $\cos(\varphi_1) = \cos(\varphi_2) = 0.95$)

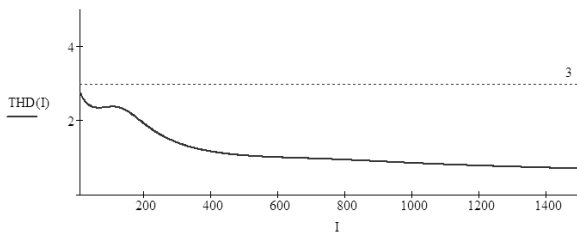


Fig. 5. THD(I) diagram ($k_1 = 0.9$, $k_2 = 1.1$, $\cos(\varphi) = 0.98$, $\cos(\varphi_1) = \cos(\varphi_2) = 0.95$)

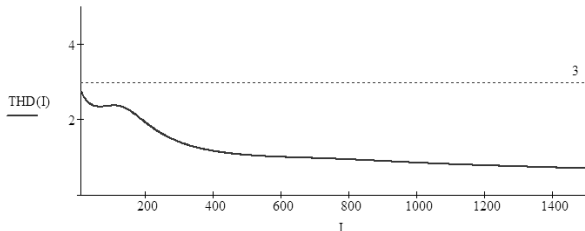


Fig. 6. THD(I) diagram ($k_1 = 0.9$, $k_2 = 1.1$, $\cos(\varphi) = 0.98$, $\cos(\varphi_1) = \cos(\varphi_2) = 0.85$)

Let us now look at more considerable amplitude asymmetry $k_1 = 0.8$, $k_2 = 1.2$. In the absence of phase asymmetry $\cos(\varphi) = \cos(\varphi_1) = \cos(\varphi_2) = 0.98$. THD(I) diagram will look as shown in fig. 7. In this case, three resonances are present, two of which being quite significant. Even a slight phase asymmetry $\cos(\varphi) = 0.98$, $\cos(\varphi_1) = \cos(\varphi_2) = 0.95$ does considerably improve the situation (fig. 8), but its growth, as opposed to a slight amplitude asymmetry, results in a considerable growth of THD (fig. 9).

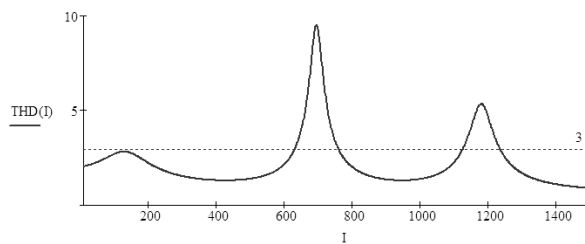


Fig. 7. THD(I) diagram ($k_1 = 0.8$, $k_2 = 1.2$, $\cos(\varphi) = \cos(\varphi_1) = \cos(\varphi_2) = 0.98$)

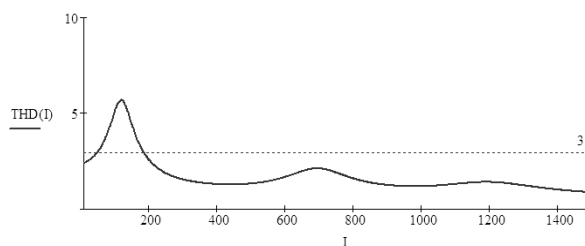


Fig. 8. THD(I) diagram ($k_1 = 0.8$, $k_2 = 1.2$, $\cos(\varphi) = 0.98$, $\cos(\varphi_1) = \cos(\varphi_2) = 0.95$)

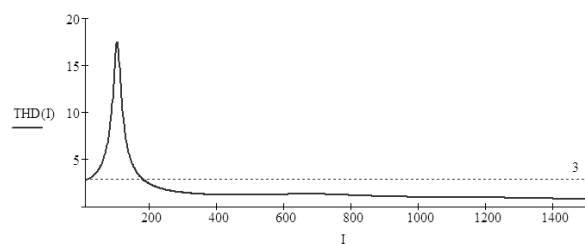


Fig. 9. THD(I) diagram ($k_1 = 0.8$, $k_2 = 1.2$, $\cos(\varphi) = 0.98$, $\cos(\varphi_1) = \cos(\varphi_2) = 0.9$)

Let us see what happens if power coefficients are different for each phase. In such a case it is also better, when the phase with a greater amplitude has lesser $\cos(\varphi)$ (fig. 10).

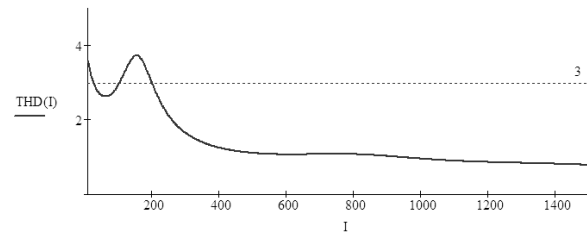


Fig. 10. THD(I) diagram ($k_1 = 0.8$, $k_2 = 1.2$, $\cos(\varphi) = 0.98$, $\cos(\varphi_1) = 0.95$, $\cos(\varphi_2) = 0.85$)

Let us consider the influence produced on THD(I) by the filter's inductance values L_1 . For $L_1 = 80\mu\text{H}$, with amplitude asymmetry of $k_1 = 0.8$, $k_2 = 1.2$ and in the absence of phase asymmetry $\cos(\varphi) = \cos(\varphi_1) = \cos(\varphi_2) = 0.98$. THD(I) diagram is presented in fig. 11.

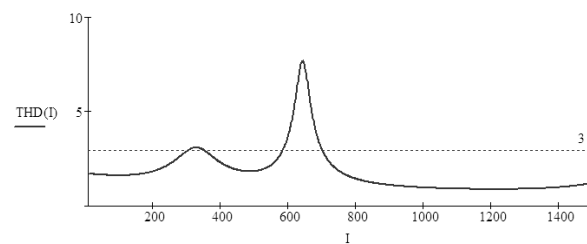


Fig. 11. THD(I) diagram ($L_1 = 80\mu\text{H}$, $k_1 = 0.8$, $k_2 = 1.2$, $\cos(\varphi) = \cos(\varphi_1) = \cos(\varphi_2) = 0.98$)

This is somewhat better than for $100\mu\text{H}$, yet not sufficient to fulfill $\text{THD} \leq 3\%$ condition. Under such conditions, the diagram looks much better for $L_1 = 60\mu\text{H}$ (fig. 12).

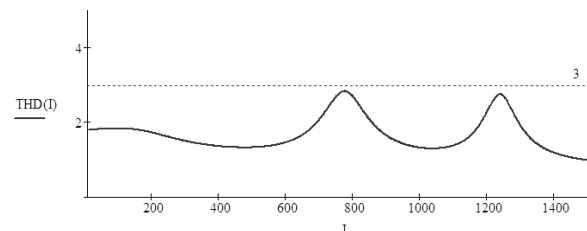


Fig. 12. THD(I) diagram ($L_1 = 60\mu\text{H}$, $k_1 = 0.8$, $k_2 = 1.2$, $\cos(\varphi) = \cos(\varphi_1) = \cos(\varphi_2) = 0.98$)

Let us now consider the influence produced on THD for 80 and $60\mu\text{H}$ inductances of slight phase asymmetry. In comparison with $100\mu\text{H}$ inductance (fig. 7), $80\mu\text{H}$ inductance generates an exceptionally high resonant current (fig. 13), under which THD reaches 40%.

For inductance of $60\mu\text{H}$, the resonance is quite moderate (fig. 14).

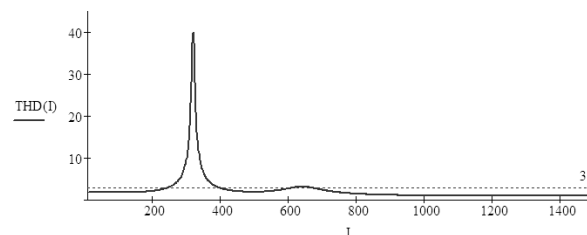


Fig. 13. THD(I) diagram ($L_1 = 80\mu\text{H}$, $k_1 = 0.8$, $k_2 = 1.2$, $\cos(\varphi) = \cos(\varphi_1) = \cos(\varphi_2) = 0.95$)

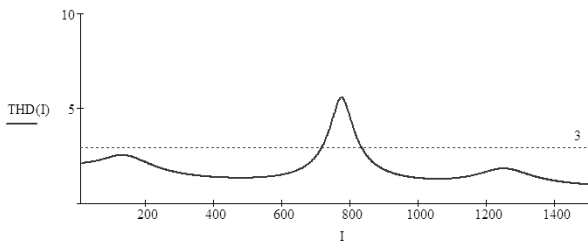


Fig. 14. THD(I) diagram ($L_1 = 60\mu\text{H}$, $k_1 = 0.8$, $k_2 = 1.2$, $\cos(\varphi) = 0.98$, $\cos(\varphi_1) = \cos(\varphi_2) = 0.95$)

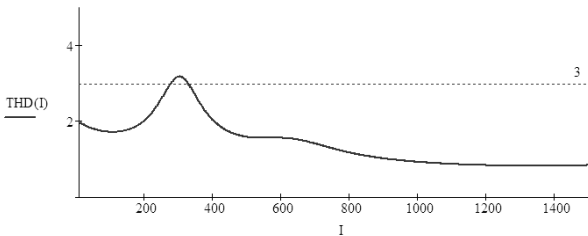


Fig. 15. THD(I) diagram ($L_1 = 80\mu\text{H}$, $k_1 = 0.8$, $k_2 = 1.2$, $\cos(\varphi) = 0.98$, $\cos(\varphi_1) = \cos(\varphi_2) = 0.9$)

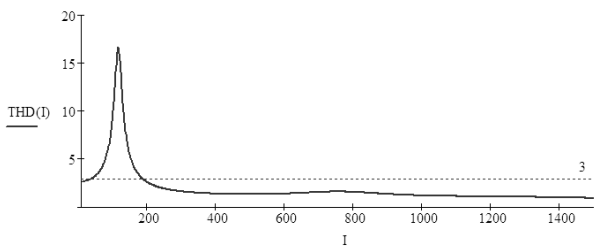


Fig. 16. THD(I) diagram ($L_1 = 60\mu\text{H}$, $k_1 = 0.8$, $k_2 = 1.2$, $\cos(\varphi) = 0.98$, $\cos(\varphi_1) = \cos(\varphi_2) = 0.9$)

When power coefficients are different for each phase, this is also better when the phase with a greater amplitude has lesser $\cos(\varphi)$ (fig. 17, fig. 18).

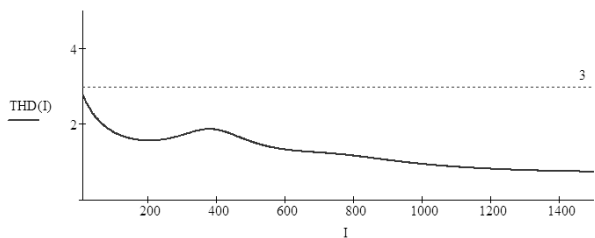


Fig. 17. THD(I) diagram ($L_1 = 80\mu\text{H}$, $k_1 = 0.8$, $k_2 = 1.2$, $\cos(\varphi) = 0.98$, $\cos(\varphi_1) = 0.95$, $\cos(\varphi_2) = 0.85$)

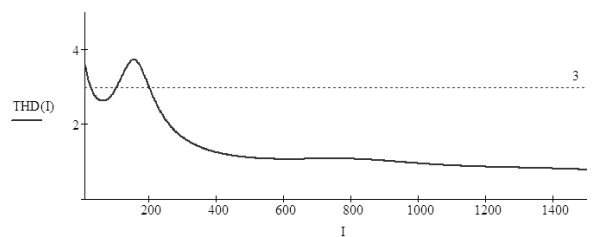


Fig. 18. THD(I) diagram ($L_1 = 60\mu\text{H}$, $k_1 = 0.8$, $k_2 = 1.2$, $\cos(\varphi) = 0.98$, $\cos(\varphi_1) = 0.95$, $\cos(\varphi_2) = 0.85$)

When analyzing the diagrams (fig. 3 – fig. 17) one can conclude that there is no uniform value of inductance L_1 , which would guarantee fulfillment of $THD \leq 3\%$ condition for all load current values and all asymmetrical modes. At the same time, there always is an opportunity to choose such C capacity that would ensure this condition for different L_1 .

For example, if for $L_1 = 80\mu\text{H}$ $C = 600\mu\text{F}$ (which corresponds to 200 μF capacity connected with a triangle) THD(I) dependency looks like in fig. 11, then simple reduction of capacity down to 450 μF (which corresponds to 150 μF capacity connected with a triangle) produces the diagram shown in fig. 19.

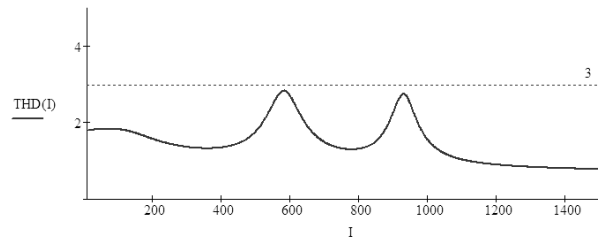


Fig. 19. THD(I) diagram ($C = 150\mu\text{F}$, $L_1 = 80\mu\text{H}$, $k_1 = 0.8$, $k_2 = 1.2$, $\cos(\varphi) = \cos(\varphi_1) = \cos(\varphi_2) = 0.98$)

There exists another possibility for restriction of resonant currents (as well as THD), and namely: to plug limiting resistors R_C into the linear wires that energize the filter's capacitor battery (fig. 20). Such being the case, one

can write as follows: $Z_2(j\omega) = \frac{1}{j\omega C} + R_C$.

Let us consider the influence produced by limiting resistors R_C on THD(I) dependency.

For $L_1 = 80\mu\text{H}$ with amplitude asymmetry of $k_1 = 0.8$, $k_2 = 1.2$ and in the absence of phase asymmetry, $\cos(\varphi) = \cos(\varphi_1) = \cos(\varphi_2) = 0.98$ (fig. 11) it is sufficient to turn on $R_C = 0.5\Omega$ to obtain $THD \leq 3\%$ (fig. 21).

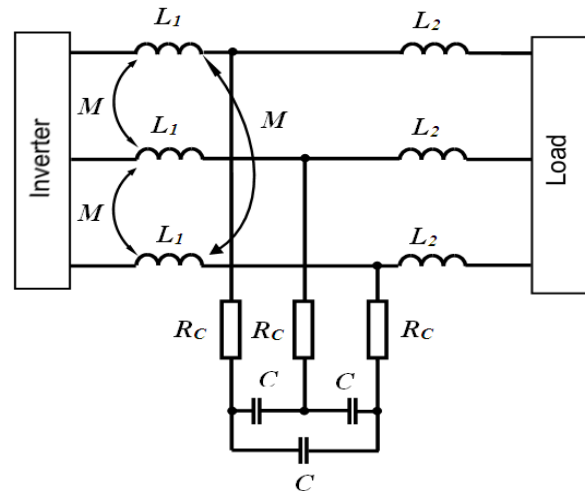


Fig.20 – Circuit of LCL-filter with limiting resistors

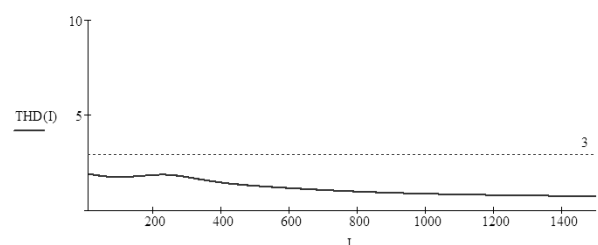


Fig. 21. THD(I) diagram ($C = 600\mu\text{F}$, $L_1 = 80\mu\text{H}$, $k_1 = 0.8$, $k_2 = 1.2$, $\cos(\varphi) = \cos(\varphi_1) = \cos(\varphi_2) = 0.98$, $R_C = 0.05\Omega$)

Amplitude asymmetry is more significant (for example $k_1 = 0.6$, $k_2 = 1.4$), such R_C value is no longer helpful (fig. 22) and should be increased to $R_C = 0.8\Omega$ (fig. 23).

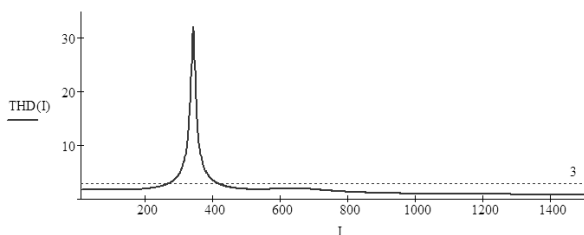


Fig. 22. THD(I) diagram ($C = 600\mu\text{F}$, $L_1 = 80\mu\text{H}$, $k_1 = 0.6$, $k_2 = 1.4$, $\cos(\varphi) = \cos(\varphi_1) = \cos(\varphi_2) = 0.98$, $R_C = 0.05\Omega$)

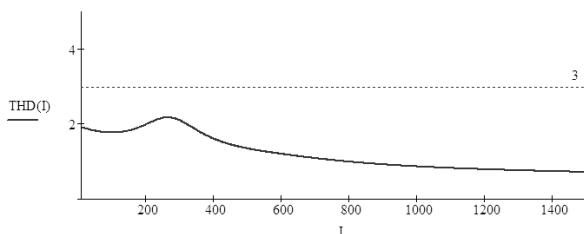


Fig. 23. THD(I) diagram ($C = 600\mu\text{F}$, $L_1 = 80\mu\text{H}$, $k_1 = 0.8$, $k_2 = 1.2$, $\cos(\varphi) = \cos(\varphi_1) = \cos(\varphi_2) = 0.98$, $R_C = 0.08\Omega$)

The use of resistors to restrict THD has a disadvantage: since current of about 40 – 50A flows through the capacity, resistors at all three phases generate total heat of 400 – 600W. Taking into account the requirements applicable to filter compactness, such a power impairs the filter's heat balance, which may cause unwanted consequences. Hence, in order to fulfill $THD \leq 3\%$ condition for all loads, since automatic regulation of inductance value is much more difficult than that of capacity value, it is advisable to choose a certain optimal inductance that would satisfy most network modes, and to achieve this condition in one of the two following ways:

- by regulating the filter's capacity;
- by regulating the active supports of limiting resistors, where there is a possibility to ensure cooling of the filter.

Conclusions

Stable operation of present-day solar power plants is ensured by availability of accumulator batteries being charged at night from the network, so for the reverse mode of inversion systems' operation it is advisable to use LCL-filters.

In order to reduce the dimensions and the cost of LCL-filters, it is advisable to design them as a three-leg magnetic system having magnetic coupling between inductances of different phases. There is no uniform value of LCL-filter's inductance that would guarantee fulfillment of $THD \leq 3\%$ condition for all values of load current and all modes (symmetrical or asymmetrical), therefore it is advisable to choose a certain optimal inductance that would satisfy most network modes, and to achieve this condition automatically by regulating either the filter's capacity or active supports of limiting resistors (if installed).

Authors: Vasyl V. Kukharchuk, Vinnytsia National Technical University, Khmelnytsky highway, 95, 21000, Vinnytsia, Ukraine, Samoil Sh. Katsyv, Vinnytsia National Technical University, Khmelnytsky highway, 95, 21000, Vinnytsia, Ukraine, Valerii F. Hraniak, Vinnytsia National Technical University, Khmelnytsky highway, 95, 21000, Vinnica, Ukraine, e-mail: titanxp2000@ukr.net, Vyacheslav G. Madyarov, Vinnytsia National Technical University, Khmelnytsky highway, 95, 21000, Vinnytsia, Ukraine, E-mail: titanxp2000@ukr.net, Volodymyr V. Kyivskiy, LLC «KNESS RND CENTER», str. Energetychna, 5A, 21022, Vinnitsia, Ukraine, Ph.D, Associate Professor, Iryna V. Prychepa, Vinnytsia National Technical University, 95 Khmelnytske shose, Vinnytsia, Ukraine, 21021, E-mail: prychepa.iryana@gmail.com, dr hab. inż. Andrzej Kotyra, Instytut Elektroniki i Technik Informacyjnych, Politechnika Lubelska, ul. Nadbystrzycka 38a, 20-618 Lublin, Poland, a.kotyra@pollub.pl, Bakhyt Yerallyeva, Taraz State University after M.Kh.Dulaty, Taraz, Kazakhstan, E-mail: b_eral@mail.ru, Ainur Kozbakova, Institute of Information and Computational Technologies CS MES RK, University of Power Engineering and Telecommunications Almaty, Kazakhstan E-mail: ainur79@mail.ru

REFERENCES

- [1] Sazonov, A.S., Lebedev, D.Y., Calculation and selection of parameters of sinus filters of frequency-controlled drives with a PWM voltage inverter, *Industrial energy*, 2 (2012), 18-22
- [2] Klimov V.P., Modern directions of development of AC power converters, *Practical Power Electronics*, 5 (2007), 43-51
- [3] Chen S., Lai Y.M., Tan S-Ch., Tse Ch.K., Optimal Design of Repetitive Controller for Harmonic Elimination in PWM Voltage Source Inverters, *Proceedings on 29th International Telecommunications Energy Conference* (2007), 236-241
- [4] Eid A., El-Kishky H., Abdel-Salam M., El-Mohandes T., VSCF aircraft electric power system performance with active power filters, *Proc. on 42th Southeastern Symposium of System Theory (SSST) 2010*, 182-187
- [5] Anuchin A.S., Kulmanov I.I., Belyakov Y.O., Compensation of harmonic distortion of the output voltage in power supplies with a sinus filter, *Proceedings of the VIII International Conference on Automated Electric Drives AED-2014*, vol. 1 (2014), 93-98
- [6] Pustovetov M.Y., Calculation of parameters and computer simulation of sinus filters in a variable frequency drive, *Bulletin of DSTU*, 3(64) (2012), 56-64.
- [7] Hraniak V.F., Kukharchuk V.V., Bilichenko V. V. et al., Correlation method for calculation of weight coefficients of artificial neural-like networking hydraulic units' diagnostic systems, *Proceedings of SPIE 11176, Photonics Applications in Astronomy, Communications, Industry and High-Energy Physics Experiments* (2019), 1117663
- [8] Vedmitskiy Y.G., Kukharchuk V.V., Hraniak V.F. et al., Newton binomial in the generalized Cauchy problem as exemplified by electrical systems, *Proceedings of SPIE 10808, Photonics Applications in Astronomy, Communications, Industry, and High-Energy Physics Experiments 2018 – 7 p.*
- [9] Vasilevskiy, O.M. Calibration method to assess the accuracy of measurement devices using the theory of uncertainty, *International Journal of Metrology and Quality Engineering*, 5(4) (2014), 47-53
- [10] John M., Mertens A., Harmonic domain model of an open-loop controlled PWM converter *Informatyka, Automatyka, Pomiar w Gospodarce i Ochronie Środowiska*, 8(2) (2018), 25-29.
- [11] Grzejszczak P., Barlik, R., Leszczyński, B., Szymczak M., Investigation of a high-efficiency and high-frequency 10-kW/800-V three-phase PWM converter with direct power factor control, *International Journal of Electronics and Telecommunications* 65(4) (2019), 619-624